DESIGN OF A RESONATOR FOR THE CSU THz FEL

P.J.M. van der Slot,*

University of Twente, Mesa$^+$ Institute for Nanotechnology, Enschede, The Netherlands
Colorado State University, Department of Electrical and Computer Engineering, Fort Collins, USA
S.G. Biedron and S.V Milton,
Colorado State University, Department of Electrical and Computer Engineering, Fort Collins, USA

Abstract

A typical confocal resonator for THz radiation produced by an FEL will have a waist that is larger than the gap of the undulator. Hence waveguiding is required. Here we consider a resonator consisting of two spherical mirrors and a cylindrical waveguide in between. The radii of curvature for the mirrors are chosen to image the ends of the waveguide onto themselves. We discuss the properties of the cold resonator for a wavelength range from 200 to 600 μm and show that the outer radii of the mirrors can be used to control the mode content inside the cylindrical waveguide.

INTRODUCTION

The field of TeraHertz (THz) radiation, which fills the so-called frequency gap between 0.1 and 10 THz (30 μm to 1 mm), has seen significant progress in recent years [1]. The unique properties of THz radiation, together with source and diagnostic developments have enabled applications in medical sciences, non-destructive evaluation, homeland security, control of food quality and in many other areas. Despite the progress, sources with high peak power of 100 kW or more are still lacking. The Colorado State University Accelerator Facilty [2] aims to study, amongst others, various ways to efficiently generate high peak power THz radiation using a FEL. The THz FEL consists of a 6 MeV, L-band, linear accelerator and a fixed gap, equal focussing, linear undulator with $N_u = 50$ periods of $\lambda_u = 2.5$ cm length. The wavelength of this system varies from approximately 200 to 600 μm.

Operating at THz frequencies requires wave guiding to avoid excessive diffraction losses [3]. Usually, parallel plate waveguiding is used, where guiding is provided in one plane and free-space propagation in the other [3, 4]. The effect of cylindrical waveguides on the optical mode propagation has been considered for far-infrared FELs where the wavelengths are such that optical propagation through the cylindrical beam pipe inside the undulator borders between free-space propagation and guided wave propagation [5]. Ref. [5] shows that for sufficiently small wavelengths, the cylindrical waveguide could be replaced by two apertures at the waveguide ends without modifying the wave propagation. At larger wavelengths, the study shows that for the waveguide the optical mode is modified and the roundtrip loss drops below the loss when the waveguide is replaced

---
* p.j.m.vanderslot@utwente.nl

by two apertures. In order to model the field inside the waveguide, both TE and TM modes were required.

For the CSU THz FEL, the wavelengths are significantly longer and using a resonator consisting only of spherical mirrors would result in a waist diameter that is larger than the gap of the undulator. We therefore consider a geometry where a cylindrical waveguide is used to "image" the waist from one end of the waveguide to the order end. The minimum length of the waveguide is the physical length L_u of the undulator, $L_u = 1.35$ m (note, this is longer than $N_u \lambda_u$). The resonator is completed by two spherical mirrors positioned at either end of the waveguide. Distance and radius of curvature (focal length) are chosen such that the mirror images the end facet of waveguide on to itself. Since the FEL will produce linearly polarised light, it is sufficient to only include TE modes for describing the field inside the waveguide. The resonator is analysed using the Fox-Li method [6]. In the remainder of this paper we first discuss the coupling of a fundamental Gaussian mode to the waveguide and then discuss the properties of the resonator.

COUPLING OF A GAUSSIAN MODE TO A WAVEGUIDE

The resonator consists of a cylindrical waveguide with two spherical mirrors on either side. Propagation of the optical field inside this resonator consists of guided wave propagation inside the waveguide and free-space propagation in between the waveguide ends and the mirrors. It is therefore of interest to determine the coupling of the free-space optical field to the TE_{nm} waveguide modes, which are the only modes of interest for the chosen geometry. The electric field of a linear polarised optical field inside the waveguide can be written as a superposition of TE_{nm} modes as (cylindrical coordinates r, ϕ, z)

$$\mathbf{E}(r, \phi, z, t) = \sum_{n,m} B_{nm} \mathbf{E}_{nm}(r, \phi) e^{i(\omega t - \beta_{nm} z)} \quad (1)$$

where

$$\mathbf{E}_{nm}(r, \phi) = i\frac{nk_0 Z_0}{r} J_n(\kappa_{nm} r) sin(n\phi)\hat{r} \\ + ik_0 Z_0 \kappa_{nm}\beta_{nm} J_n'(\kappa_{nm} r) cos(n\phi)\hat{\phi}. \quad (2)$$

In eqs. 1 and 2, B_{nm} is the mode amplitude, $\omega = ck_0$, c being the speed of light in vacuum, $k_0 = \frac{2\pi}{\lambda}$, λ being the free-space wavelength, Z_0 is the vacuum impedance, $\beta_{nm} = \sqrt{k_0^2 - \kappa_{nm}^2}$ is the propagation constant of the
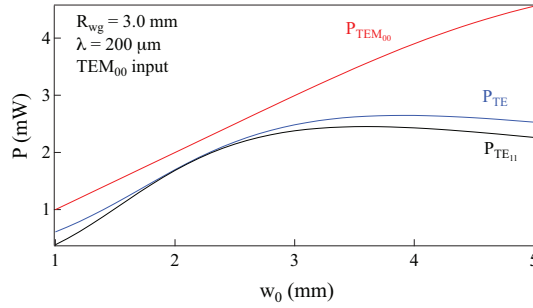
Figure 1: Coupling between free-space Gaussian TEM_{00} mode and the TE_{nm} modes in a cylindrical waveguide of radius $R_{wg} = 3.0\,\mathrm{mm}$.

Figure 2: Optical field intensity (E_x) at the end of the waveguide when a TEM_{00} mode with $\lambda = 200\,\mu\mathrm{m}$ and $w_0 = 2.8\,\mathrm{mm}$ is incident on the other side for $L_{wg} = 2.5524\,\mathrm{m}$ (A) and $L_{wg} = 1.9134\,\mathrm{m}$ (B).

mode, J_n is the Bessel function of the first kind of order n, $\kappa_{nm} R_{wg}$ is the mth root of $J_n'(x) = 0$, the prime indicates the derivative with respect to its argument, and R_{wg} is the radius of the waveguide. The coefficients B_{nm} can be calculated through

$$B_{nm} = -c_{nm} \int_S \mathbf{E} \cdot \mathbf{E}_{nm} dS, \qquad (3)$$

with

$$c_{nm} = \left[\omega^2 \epsilon_{0n} \pi \frac{a_{nm}^2}{2} \left(1 - \frac{n^2}{a_{nm}^2} \right) J_n^2(a_{nm}) \right]^{-1}, \qquad (4)$$

$a_{nm} = \kappa_{nm} R_{wg}$, ϵ_{0n} equals 1 when $n=0$ and 2 otherwise, and the integration is over the cross section S of the waveguide. As the ratio of the wave impedance Z inside the waveguide to the wave impedance Z_0 in free space is given by $\frac{k_0}{\beta_{nm}}$ [7], and $\beta_{nm} \approx k_0$, we ignore reflections when the waveguide mode is emitted in free space. Furthermore, we assume the waveguide wall to be a perfect conductor.

As an example we consider a Gaussian TEM_{00} mode that is focused on the end of a waveguide. Unless otherwise specified, the radius of the waveguide is $R_{wg} = 3\,\mathrm{mm}$. We use Eq. 3 to calculate the mode amplitudes in the waveguide as a function of the waist w_0 of the Gaussian mode (1/e value for the electric field), where the peak intensity of the mode is kept constant. Figure 1 shows the total power in the TEM_{00} mode, which increases with w_0, the power in the lowest order TE_{11} waveguide mode, $P_{TE_{11}}$, and the power in all TE_{nm} modes together, P_{TE}, ($n \le 5, m \le 20$). We observe that for $w_0 = 2.4\,\mathrm{mm}$ the coupling is maximum at 87.6 % and for $2.0\,\mathrm{mm} < w_0 < 2.4\,\mathrm{mm}$ less than 1 % of the energy is in higher order modes, i.e. only the TE_{11} mode is excited. For smaller and larger w_0, the coupling to the waveguide modes decreases and higher order modes are excited.

If the incident field excites a single mode at the entrance of the waveguide, then this mode will be radiated in free space at the other side. On the other hand, if an incident field excites multiple modes at the waveguide entrance, the modes will propagate with slightly different propagation constants β_{nm} and consequently are generally not in
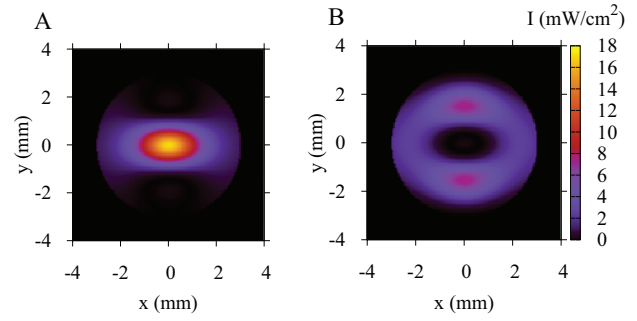
phase any more at the exit of the waveguide. Therefore, the electric field distribution at the exit will generally be different from that at the entrance. This is illustrated in Fig. 2 where the intensity from the E_x component of the field at the exit of the waveguide is shown for two different length of the waveguide, $L_{wg} = 2.5524\,\mathrm{m}$ (Fig. 2a) and $L_{wg} = 1.9134\,\mathrm{m}$ (Fig. 2b), for a TEM_{00} mode with $\lambda = 200\,\mu\mathrm{m}$ and $w_0 = 2.8\,\mathrm{mm}$ incident on the other side of the waveguide. For this case, the energy contained in the 4 lowest TE_{1m} modes is 0.493, 0.189, 0.015 and 0.003 mW respectively (m=1,2,3,4). For a length of $L_{wg} = 2.5524\,\mathrm{m}$ the modes m=1,2 and 3 are in phase and the field distribution inside the waveguide at its entrance is reproduced at its exit (see Fig. 2a). Note, the although the other modes are not in phase with the first three modes, the energy in these modes is so low that they can be neglected. On the other hand, for a length of $L_{wg} = 1.9143\,\mathrm{m}$ the modes m=1 to 4 are no longer in phase which each other and interference between the modes significantly changes the field distribution at the exit (see Fig. 2b). The constructive interference shown in Fig. 2a repeats itself for waveguide lengths that are an integer multiple of $L_{wg,0} = 1.2762\,\mathrm{m}$. The length $L_{wg,0}$ depends on the propagation constants β_{nm} and is thus wavelength dependent. For a wavelength of $\lambda = 600\,\mu\mathrm{m}$, $L_{wg,0}$ equals 1.2201 m. Again, only the three lowest TE_{1m} modes are in phase. Note, if one would require the four lowest TE_{1m} to be in phase, the waveguide should be 105.9 m and 1106.6 m long for $\lambda = 200$ and $600\,\mu\mathrm{m}$, respectively. Also, at intermediate wavelengths $L_{wg,0}$ can be considerably larger, even more than an order of magnitude.

To conclude, for THz frequencies, an overmoded waveguide can transpose an input optical field for specific lengths of the waveguide as long as the incident field only excites a few modes at most. A single mode will always be transposed for any value of L_{wg}. For the case studied here, the three lowest TE_{1m} modes constructively interfere for a particular waveguide length $L_{wg,0}$, which may vary considerably with the wavelength. As we show in the next section, it is still possible to use a cylindrical waveguide
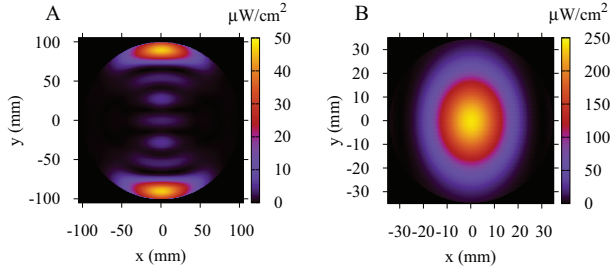
Figure 3: Intensity of the optical field (E_x) incident at the downstream mirror for $\lambda = 200\,\mu m$ and $R_{o,dn} = R_{o,up} = 100\,mm$ (A) and $R_{o,dn} = 34.5\,mm$ and $R_{o,up} = 17.5\,mm$ (B). The hole radii are $R_{h,dn} = 5\,mm$ and $R_{h,up} = 2\,mm$.

Figure 4: Intensity from the E_x component of the optical field incident at the upstream side of the waveguide for $\lambda = 200\,\mu m$ and $R_{h,dn} = 5\,mm$ (A) and $R_{h,dn} = 25\,mm$ (B). Other parameters as for Fig. 3b.

in a resonator by controlling the mode content inside the waveguide.

FOX-LI ANALYSIS OF THE RESONATOR

The CSU THz FEL is driven by an L-band linac that can produce a maximum energy of 6 MeV. The electron bunches are generated using a photocathode that is driven by the third harmonic of a Ti:Sapphire laser capable of producing 30 fs to around 1 ps pulses at a repetition rate of $f_{rep} = 81.25\,MHz$ (16th subharmonic of linac frequency). The condition for overlap between the electron bunches and the recirculating optical pulse in the resonator is

$$L_{res} = \frac{1}{2}ct_{rep} = \frac{c}{2f_{rep}}, \qquad (5)$$

or an integer times this value. Here, t_{rep} is the time between two consecutive electron bunches, L_{res} is the length of the resonator, and we ignore the difference in phase velocity of the optical field inside the waveguide and in vacuum. Using Eq. 5 we find that the minimum length for the resonator is 1.8449 m. In view of the required length of the waveguide to transpose an optical field from the upstream end to the downstream end (up- and downstream are defined with respect to the e-beam propagation through the resonator), we consider a resonator length that is twice as long, $L_{res} = 3.6898\,m$. For the downstream mirror we take a radius of curvature of $R_{c,dn} = 75\,cm$, which places the mirror at a distance of $d_{dn} = 2f_{dn} = R_{c,dn}$ from the waveguide end in order to image the waveguide end onto itself. Here $f_{dn} = R_{c,dn}/2$ is the focal length of the downstream mirror. We set the waveguide length to $L_{wg} = 2.5524\,m$, i.e. equal to $2L_{wg,0}$ for $\lambda = 200\,\mu m$. Consequently, the radius of curvature for the upstream mirror is then $R_{c,up} = 38.75\,cm$ with a distance of $d_{up} = R_{c,up}$ to the waveguide. This resonator is analysed using the so-called Fox-Li method [6], where an initial field (in our case a TEM_{00} mode) is tracked [8] through the resonator for a number of roundtrips until a stationary optical distribution is obtained. To compensate for losses in the resonator, the power of the optical field incident on the upstream side of the waveguide is reset to a value of 2.8 mW (the power in the initial TEM_{00} mode) at the start of each new roundtrip.
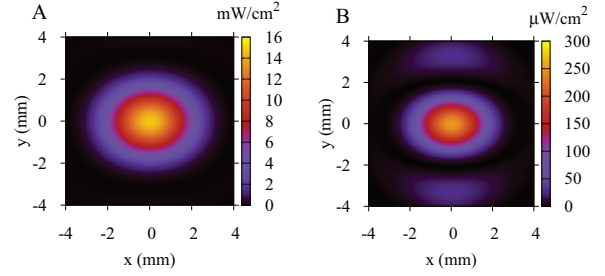
Ideally, one would like to keep L_{wg} equal to $2L_{wg,0}(\lambda)$ when the FEL is tuned from 200 to 600 μm. However, as this length varies wildly over the wavelength range, implementation is not pratical. Even for $\lambda = 200\,\mu m$, the presence of holes in the mirrors can results in significant diffraction and excitation of higher order modes in the waveguide that results in different optical distributions on either side of the waveguide. This is illustrated in Fig. 3a, where the intensity from the E_x component incident on the downstream mirror is plotted for the outer radii of the mirrors equal to $R_{o,dn} = R_{o,up} = 100\,mm$. The stationary intensity distribution shown in Fig. 3a corresponds to only 0.2 % of the optical energy inside the waveguide to be in the TE_{11} mode, while the remainder of the energy is distributed over higher order TE_{nm} modes. A total of $n \leq 5$ and $m \leq 20$ modes were included in the calculation. The higher order TE modes will experience a larger diffraction. In this particular example the outer radii of the mirrors are sufficiently large to still largely reflect the diffracted field of these higher order modes. By restricting the outer radii of the mirrors, the losses for the higher order modes are increased. This can be used to prevent the build-up of higher order modes, i.e., the amplification of the optical field at the start of each roundtrip to reset the power equal to 2.8 mW is less than the roundtrip losses for the higher order modes. For example, when $R_{o,dn}$ is reduced to 37.5 mm and $R_{o,up}$ to 17.5 mm, a stationary intensity distribution as shown in Fig. 3b is found. For these radii, 98.4 % of the optical energy inside the waveguide is in the TE_{11} mode. Note, that the optical field is confined to a much smaller area and has an elliptical shape. The later is due to the fact that the field distribution of the TE_{11} mode is narrower in the y-direction than in the x-direction (see Fig. 2a). Consequently the diffraction in the y-direction is larger and an elliptical profile results. A very similar behaviour is observed if the wavelength is increased to 600 μm, albeit with different outer radii of the mirrors. We therefore will only present results for $\lambda = 200\,\mu m$.

The radiation is coupled out of the resonator through the hole in the downstream mirror. It remains to be seen up to which hole radius this method of control over the mode content inside the waveguide remains effective. Fig. 4
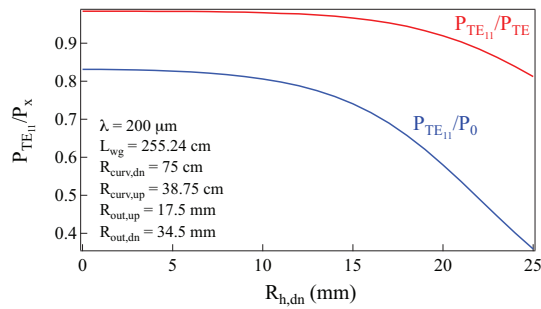
Figure 5: Ratio of the power $P_{TE_{11}}$ to P_0 and to P_{TE} as a function of $R_{h,dn}$.

Figure 6: $P_{h,dn}/P_0$, $P_{h,dn}/P_{m,dn}$ and $P_{h,dn}/P_{loss}$ as a function of $R_{h,dn}$. P_0=2.8 mW.

shows the stationary intensity distribution at the upstream waveguide end at the end of a roundtrip for $R_{h,dn} = 5\,\mathrm{mm}$ (A) and $R_{h.dn} = 25\,\mathrm{mm}$ (B). The other parameters are identical to the case shown in Fig. 3b. The difference in optical intensity is due to the much larger fraction of the radiation being coupled out of the resonator for the larger hole radius. For the case $R_{h,dn} = 5\,\mathrm{mm}$, about 98.4 % of the optical energy inside the waveguide is in the TE_{11} mode, while this fraction is 81.2 % for $R_{h.dn} = 25\,\mathrm{mm}$ (see Fig. 5). The larger higher order mode content is clearly visible both in the intensity distribution at the upstream side of the waveguide (Fig. 4b) as well as from the ratio of the power in the TE_{11} mode to the total power in all modes (Fig. 5). Fig. 4b shows that the central field distribution narrows and side lobes appear that fall outside the waveguide aperture. This distribution results in a lower coupling to the waveguide modes and increased losses (cf. Fig. 5). For both cases, the intensity distribution at the downstream mirror looks very similar as shown in Fig. 3b. Comparing Fig. 4a to Fig. 2a shows that the stationary field incident at the upstream side of the waveguide is not exactly that of a TE_{11} mode. As the small outer radii of the mirrors suppress the higher order modes by increasing the diffraction losses, also the TE_{11} mode will experience diffraction losses and these losses are primarily responsible for the change in the intensity profile when the optical field propagates from the waveguide end to the mirror and back.

In Fig. 5 we plot the ratio of the power extracted through the hole in the downstream mirror, $P_{h,dn}$, to the initial power at each roundtrip, P_0 (=2.8 mW), to the power incident on the surface of the downstream mirror, $P_{m,dn}$ and to the total power lost over one roundtrip, P_{loss}, as a function of the hole radius $R_{h,dn}$. We see that the largest fraction of the incident power is coupled out of the resonator for $R_{h,dn} \approx 18\,\mathrm{mm}$, while the largest fraction of the total roundtrip loss coupled out of the resonator is for $R_{n.dn} \approx 16\,\mathrm{mm}$. The total roundtrip loss is 94 and 91 %, respectively. The maximum in $P_{h,dn}/P_0$ coincides with the appearance of side lobes in the field incident on the upstream end of the waveguide, i.e., with the appearance of higher order order modes inside the waveguide (cf. Figs. 4b and 5).
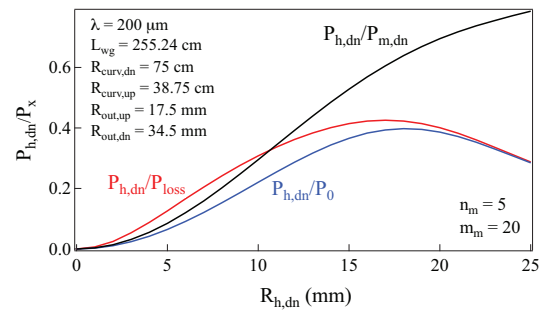
DISCUSSION AND CONCLUSIONS

We have shown that by controlling the outer radii of the spherical mirrors a single mode can be excited in the waveguide over a large range of radii for the hole in the downstream mirror. However this comes at the expense of large diffraction losses and therefore this configuration is only suitable for a high gain FEL, which is the case for the CSU THz FEL. More than 40 %, and possibly more than 50 % after further optimisation, of the roundtrip loss is due to power leaving the resonator through the hole in the downstream mirror. Including FEL gain may provide another mechanism to selectively amplify a single mode, and this may allow a further optimisation of the mirrors to reduce diffraction losses. This will be the subject of a future study.

ACKNOWLEDGMENT

REFERENCES

[1] M. Tonouchi, "Cutting-edge terahertz technology", Nat. Phot. **1**, p. 97 (2007).

[2] S. Milton et al., "The CSU accelerator and FEL facility", FEL'12, Nara, August 2012, WEPD03, p. 373 (2012), http://www.JACoW.org

[3] A. Amir, I. Boscolo, and L.R. Elias, "Spontaneous emission in the waveguide free-electron laser", Phys. Rev. A, **32**, p. 2864 (1985).

[4] M. Tecimer, "Numerical studies of (partial-) waveguide FELs", Nucl. Instr. and Meth. A**483**, p. 521 (2002).

[5] K.W. Berryman and T.I. Smith, "Optical modes in a partially waveguided cavity", Nucl. Instr. and Meth. A**318**, p. 885 (1992).

[6] A.G. Fox and T. Li, "Resonant modes in a maser interferometer", Bell Syst Tech J. **40**, p. 453 (1961).

[7] D.M. Pozar, *Microwave Engineering*, (Hoboken: Willey, 2012).

[8] J.G. Karssenberg et.al., "Modeling paraxial wave propagation in free-electron laser oscillators", J. Appl. Phys. **100**, 093106 (2006).